nature geoscience

Brief Communication

https://doi.org/10.1038/s41561-022-01096-w

Recovery from microplastic-induced marine deoxygenation may take centuries

Received: 15 June 2022

Accepted: 26 October 2022

Published online: 22 December 2022

Check for updates

Karin Kvale[1,2] & Andreas Oschlies[1]

Climate change and plastics pollution are dual threats to marine environments. Here we use biogeochemical and microplastic modelling to show that even if there is complete removal of microplastics and cessation of deposition in the oceans in 2022, regional recovery from microplastic-induced remineralization and water column deoxygenation could take hundreds of years for coastal upwelling zones, the North Pacific and Southern Ocean. Surface stratification and reduced sea ice cover further impede regional recovery, highlighting the importance of aggressive mitigation of plastic pollution.

Plastics are widely recognized as a persistent pollutant in the marine environment, with half-lives anywhere from decades to millennia[1]. Despite this persistence, the frequently posited solution to halting its global spread and possibly negative environmental effects is relatively simple: 'turn off the tap' or prevent plastic waste from entering the marine environment[2]. Given the long half-lives of plastics, it seems possible that contamination of the marine environment by microplastic, and its chemical constituents, is already likely to persist on the order of decades to many centuries. But, it is also possible that a long-term biogeochemical commitment has similarly been made, owing to microplastics-induced changes in the marine food web and their imprints on marine biogeochemistry that have already occurred. Our modelling framework examines the latter. Here we simulate an extreme case of such a scenario, where starting from the year 2022, all microplastic pollution of the marine environment is ceased, and all already-accumulated microplastic is instantaneously removed from the ocean. We consider microplastics as those plastics within a size range that have the potential to interact with the base of the marine food web, typically thought to be fragments below 5 mm in length[3] (Methods). In the absence of biology, these particles are thought to follow neutrally buoyant trajectories, although in practice, their global distribution may be primarily determined by their interaction with biology[4].

A recent analysis demonstrated the potential for microplastic ingestion by zooplankton to stimulate a global acceleration of deoxygenation, as the relaxation of top-down control on phytoplankton growth, owing to zooplankton replacing a fraction of their food with microplastic, can increase the production of organic particles in nutrient-replete regions such as the Southern Ocean[5]. Organic particles remineralize as they sink (a process which consumes oxygen). Water column oxygen is impacted differently in nutrient-limited regions, such as the tropical oceans and mid-latitude gyres. In these regions, recycling of nutrients in the upper ocean by zooplankton helps to maintain phytoplankton growth, thus replacing a fraction of zooplankton food with microplastics causes a decrease in organic particle production and export, and a consequential decline in oxygen consumption[5].

We explore the possibility of an oxygenation perturbation commitment due to microplastic contamination of the marine environment using the model and extended methods of ref. (5) (Methods, Extended Data Table 1 and Extended Data Fig. 4) . We find that while at a global scale, most of the microplastic-induced deoxygenation that has occurred by the year 2022 is reversible within this century (Fig. 1a), regional anomalies can persist longer (Fig. 1b). Low-latitude upwelling zones, the North Pacific and Southern Ocean all demonstrate recovery timescales that extend beyond a century. The mechanism of persistence in the Indian Ocean and North Pacific is not a retained remineralization signal (Fig. 1c) but the inhibition of air–sea gas exchange by thermal stratification of the upper ocean, a phenomenon that is enhanced by climate warming (Extended Data Fig. 1). Multi-century remineralization anomalies are retained in semi-enclosed regions such as the Gulf of Mexico and Hudson Bay.

In the Southern Ocean, water column recovery of the microplastic-induced oxygen deficit is assisted by the presence of sea ice (Figs. 1d and 2). When microplastic ingestion increases organic particle export in the nutrient-replete Southern Ocean[5] (in these experiments, between the years 1950 and 2022), additional oxygen is consumed throughout the water column by bacterial remineralization. This impacts water column oxygen, nutrients and carbon across the Southern Ocean biogeochemical divide[6]. The deep water masses rise to the

[1]Biogeochemical Modelling, GEOMAR Helmholtz Centre for Ocean Research Kiel, Kiel, Germany. [2]GNS Science, Lower Hutt, New Zealand.
e-mail: k.kvale@gns.cri.nz; aoschlies@geomar.de

https://doi.org/10.1038/s41561-022-01096-w

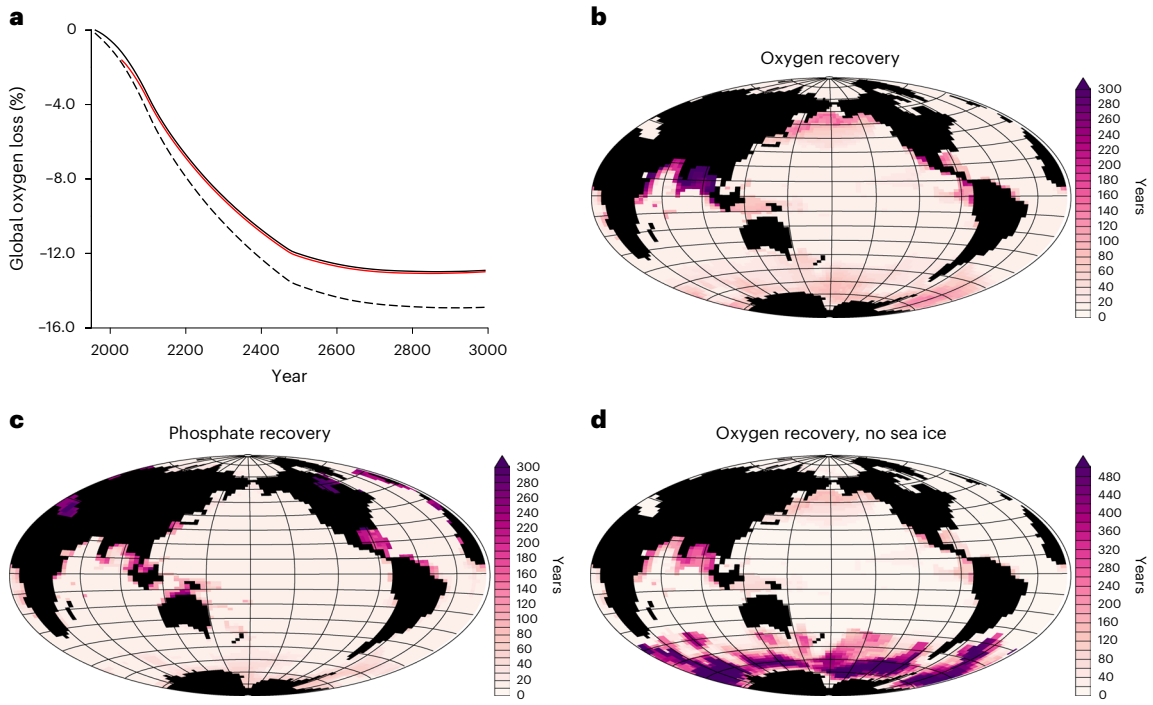

Fig. 1 | Water column recovery of microplastic-induced oxygen perturbation. **a**, Time series of global oxygen loss as a percentage relative to value at year 1950 due to climate change (solid black line), ongoing microplastic pollution (dashed black line) and microplastic removal (red line). **b**, Timescale in years of average water column oxygen recovery to within 1% of the climate change-only value (MP_{STOP}-CNTL, Methods). **c**, As with **b**, but for phosphate recovery. **d**, As with **b**, but for when sea ice does not prevent air–sea oxygen exchange (MP_{NOICE}-$CNTL_{NOICE}$, Methods).

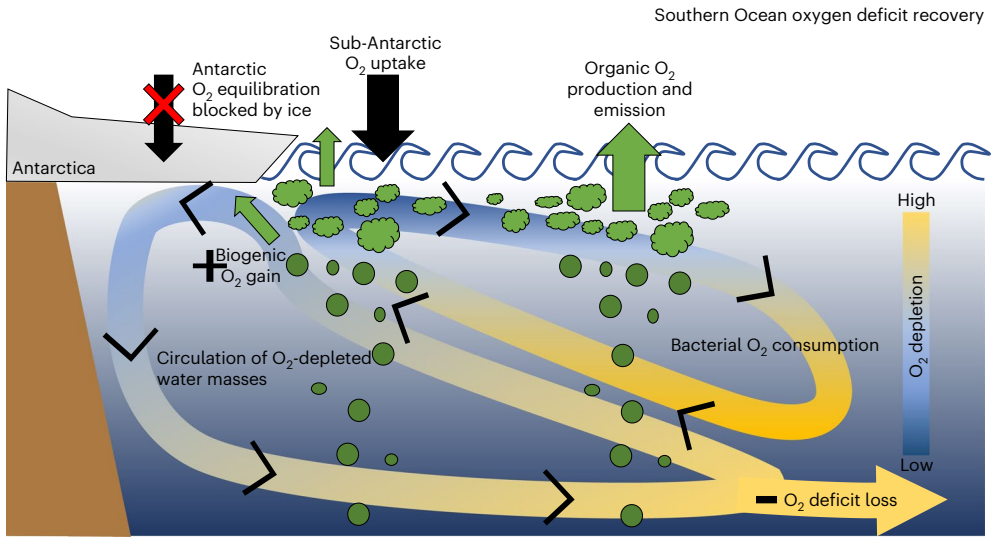

Fig. 2 | Schematic of Southern Ocean oxygen cycling. Schematic illustrates the slow recovery of the microplastic-induced oxygen deficit in the basin. Green arrows are biogenic oxygen flux, black arrows are solubility-driven oxygen fluxes, plus sign indicates an oxygen gain, minus sign indicates an oxygen deficit loss, green blobs represent phytoplankton and resulting organic detritus. Tailess arrows indicate the average direction of overturning circulation.

surface as they move south, but oxygen re-equilibration with the atmosphere is inhibited by the presence of sea ice in the southern branch of the biogeochemical divide[7]. Paradoxically, because sea ice prevents the intrusion of atmospheric oxygen into this oxygen-depleted southern branch, sea ice also provides the major mechanism of water column oxygen recovery in this region. This is because nutrient trapping due to historical microplastic contamination enhances net primary and biogenic oxygen production, the latter of which is prevented from escaping to the atmosphere by the sea ice cover. An additional sensitivity test of the oxygen deficit recovery in the complete absence of sea ice substantially extends the Southern Ocean recovery timescale to over 500 years (Fig. 1d).

These results have implications for the timing of microplastics mitigation efforts and suggest delays in efforts to curb biogeochemical effects of microplastics could have magnified consequences in a warmer, more stratified ocean with reduced sea ice cover. Simultaneously, mitigation of climate warming potentially assists the biogeochemical recovery of oceans from microplastic contamination.

While the global estimated deoxygenation commitment due to microplastic ingestion up to the year 2022 is small compared with that of climate warming[8], regional water column anomalies can continue to magnify climate-induced trends in the metabolic index[9] (that is, more than 6% by the year 2200, 178 years after microplastic removal; Extended Data Fig. 2). The metabolic index is a broad indicator of metabolic viability of a marine environment. Organism physiology is evolved to match ambient oxygen concentrations within each unique environment[10], and thus, even small shifts in the metabolic index may induce pressures that will alter these ecosystems. In our simulations, the regions demonstrating the longest oxygen perturbation recovery timescales (upwelling zones, the North Pacific and Southern Ocean) are among those that are estimated to host the largest biomass concentrations of commercially targeted fish species[11], a food source that 19% of the global population depends on for 20% of their total animal-derived nutrient intake[12].

These results furthermore highlight the previously unreported role of sea ice in both preventing the recovery of the Southern Ocean from a deoxygenation event but also in mitigating its long-term severity. With the presence of Antarctic sea ice, biogenic oxygen has a critical role in the recovery of oxygen deficits in the southern branch of the biogeochemical divide. These findings also nuance our understanding of the role of sea ice in carbon exchange, as it may serve as a barrier to CO_2 outgassing and uptake.

Our results are obtained with a model that is simplistic relative to the real ocean in all respects of physical, biogeochemical and microplastic parameterization. Historical sea ice extent is under-represented in both hemispheres, and sea ice loss is probably over-estimated[13], which might lead to an overestimate of the recovery timescales of the microplastic-induced deoxygenation legacy in the Southern Ocean. We do not simulate vertical migration of zooplankton, which is known to influence water column oxygen distributions[14], nor do we simulate buoyancy changes to zooplankton faecal pellets due to microplastic incorporation[15], both of which might influence the regional biogeochemical response to zooplankton ingestion of microplastic and the recovery. We also do not simulate the full variety of microplastic types, or phytoplankton or zooplankton types, found in the real ocean. Nevertheless, our major conclusions of century scale and longer water column oxygen recovery for several biologically important ocean regions are robust across a range of microplastic models employing a range of input rates and biological interaction parameters (Extended Data Fig. 3 and Methods) and employ established physical mechanisms (increasing upper ocean stratification, for example[16], and sea ice as a barrier to air–sea gas exchange, for example[17]).

The multi-century-scale persistence of microplastic-induced oxygen anomalies is cause for reflection on the current understanding of the impact timescales for marine litter. 'Turning off the tap'—reforming plastics use and waste management behaviours so that litter no longer enters the environment is certainly worthwhile—the unmitigated microplastics-induced deoxygenation that occurs in a high pollution, 'business-as-usual' scenario at the year 3000 is around 3% the total year 1950 global oxygen inventory (Fig. 1a). But even with complete removal of microplastics, the ocean is potentially committed to a multi-century deoxygenation legacy.

Online content

Any methods, additional references, Nature Portfolio reporting summaries, source data, extended data, supplementary information, acknowledgements, peer review information; details of author contributions and competing interests; and statements of data and code availability are available at https://doi.org/10.1038/s41561-022-01096-w.

References

1. Chamas, A. et al. Degradation rates of plastics in the environment. *ACS Sustainable Chem. Eng.* **8**, 3494–3511 (2020).
2. Owens, K.A. & Conlon, K. Mopping up or turning off the tap? Environmental injustice and the ethics of plastic pollution. Front. Mar. Sci. https://doi.org/10.3389/fmars.2021.713385 (2021).
3. Galloway, T. S., Cole, M. & Lewis, C. Interactions of microplastic debris throughout the marine ecosystem. *Nat. Ecol. Evol.* **1**, 116 (2017).
4. Kvale, K., Prowe, A. E. F., Chien, C.-T., Landolfi, A. & Oschlies, A. The global biological microplastic particle sink. *Sci. Rep.* **10**, 16670 (2020).
5. Kvale, K., Prowe, A. E. F., Chien, C.-T., Landolfi, A. & Oschlies, A. Zooplankton grazing of microplastic can accelerate global loss of ocean oxygen. *Nat. Commun.* **12**, 2358 (2021).
6. Marinov, I., Gnanadesikan, A., Toggweiler, J. R. & Sarmiento, J. L. The Southern Ocean biogeochemical divide. *Nature* **441**, 964–967 (2006).
7. Cliff, E., Khatiwala, S. & Schmittner, A. Glacial deep ocean deoxygenation driven by biologically mediated air–sea disequilibrium. *Nature Geosci.* **14**, 43–50 (2021).
8. Oschlies, A. A committed fourfold increase in ocean oxygen loss. *Nat. Commun.* **12**, 2307 (2021).
9. Deutsch, C., Penn, J. L. & Seibel, B. Metabolic trait diversity shapes marine biogeography. *Nature* **585**, 557–562 (2020).
10. Seibel, B.A. & Deutsch, C. Oxygen supply capacity in animals evolves to meet maximum demand at the current oxygen partial pressure regardless of size or temperature. J. Exp. Biol. https://doi.org/10.1242/jeb.210492 (2020).
11. Bianchi, D., Carozza, D. A., Galbraith, E. D., Guiet, J. & DeVries, T. Estimating global biomass and biogeochemical cycling of marine fish with and without fishing. *Sci. Adv.* **7**, 7554 (2021).
12. Golden, C. D. et al. Nutrition: fall in fish catch threatens human health. *Nature* **534**, 317–320 (2016).
13. Mengis, N. et al. Evaluation of the University of Victoria Earth System Climate Model version 2.10 (UVic ESCM 2.10). *Geosci. Model Dev.* **13**, 4183–4204 (2020).
14. Bianchi, D., Galbraith, E. D., Carozza, D. A., Mislan, K. A. S. & Stock, C. A. Intensification of open-ocean oxygen depletion by vertically migrating animals. *Nat. Geosci.* **6**, 545–548 (2013).
15. Cole, M. et al. Microplastics alter the properties and sinking rates of zooplankton faecal pellets. *Environ. Sci. Technol.* **50**, 3239–3246 (2016).
16. Li, G. et al. Increasing ocean stratification over the past half-century. *Nat. Clim. Change* **10**, 1116–1123 (2020).
17. Rutgers van der Loeff, M. M., Cassar, N., Nicolaus, M., Rabe, B. & Stimac, I. The influence of sea ice cover on air–sea gas exchange estimated with radon-222 profiles. *J. Geophys. Res.: Oceans* **119**, 2735–2751 (2014).

Methods

Our study uses the University of Victoria Earth System Climate Model (UVic ESCM)[18,19] in which a biogeochemical model[20,21] is embedded. The biogeochemical and microplastic models used in this study are described in ref. 4. Briefly, the biogeochemical model resolves three phytoplankton functional types: nitrogen-fixing diazotrophs, calcifiers and a generic phytoplankton. A generic zooplankton functional type grazes on the phytoplankton, organic detrital material and on itself using a Holling Type-II function that scales a maximum zooplankton grazing rate by food preference and availability. Detrital partitions simulate organic particle sinking as both particulate organic and inorganic carbon, and the organic carbon is further divided into zooplankton faecal pellet and non-pellet partitions. Faecal pellets sink and remineralize at the same rate as the non-pellet partition for simplicity. Our model does not resolve vertical migration or multiple zooplankton types, both of which are known to influence pellet sinking and biogeochemistry (for example, refs. 14, 22). Organic particles and plankton exchange nutrients with dissolved partitions of nitrate, phosphate and carbon. Alkalinity and oxygen are also traced. The microplastics model contains three microplastics tracers that are simulated as concentrations of particles for which physical characteristics such as particle size or plastic type are not resolved. Using a single, generic microplastic particle is computationally efficient but an oversimplified representation of the real ocean, which contains a wide variety of plastic particle compositions with widely varying physical characteristics, for example, ref. 23. Unattached microplastic is released via coastal grid cells and along major shipping lanes. Breakdown of large, positively buoyant plastic items in coastal zones into microplastics, which might contribute to the observed temporal lag between coastal discharge of debris and the appearance of secondary open ocean microplastics[24], is not considered. Due to the UVic ESCM's fairly coarse spatial resolution, this process is not anticipated to substantially influence our results in the present study but could be tested in the future. A fraction of the unattached microplastic is prescribed a rise rate. Unattached microplastic aggregates in marine snow (calculated using the biogeochemical model detrital production), then sinks at the rate of organic detritus as marine snow/microplastic aggregates. These aggregates are parameterized to break apart at the rate of detrital remineralization, whereupon the microplastic is released back to the unattached compartment. Similarly, zooplankton ingest both unattached microplastic and microplastic bound in marine snow aggregates, whereupon this microplastic sinks at the rate of faecal pellets and is released at the detrital remineralization rate into the unattached partition. It is assumed that ingested microplastics are inert and deliver no nutritional benefit to the zooplankton. However, microplastics can have an extensive microorganism community associated with them[25,26], although it is unclear how much nutrition they derive from it. A temperature- and oxygen-dependent maximum potential grazing rate is reduced by a scaling of total available food sources (including microplastic), weighted by a relative food preference and multiplied by the zooplankton biomass[4]. Changes to zooplankton biomass are a function of total ingested food (not including microplastic) scaled with a growth efficiency coefficient, minus mortality[4]. Alteration of the food web by the ingestion of microplastic by zooplankton occurs because while zooplankton are parameterized to graze on microplastic, this material does not contribute to their biomass. While artificial satiation via microplastic ingestion has been observed, for example, refs. 27, 28, in copepods, leading to a decline in the ingestion rate of algae, because we simulate ecosystem effects, we note a net increase in zooplankton biomass and grazing rates in nutrient-replete regions that are contaminated with microplastics and thus have phytoplankton populations that benefit from the alleviation of grazing pressure[5]. For simplicity, incorporation of microplastic into faecal pellets does not alter the sinking of the pellets in contrast to experimental evidence to the contrary, for example, ref. 15. A fraction of the microplastics bound in marine snow aggregates and faecal pellets that reach the seafloor are considered to be lost from the ocean, while the remainder are returned to the water column above the seafloor into the unattached partition. Our simple parameterization does not account for sedimentation processes that might influence microplastic sequestration[29].

The model was integrated at year 1765 boundary conditions (including agricultural greenhouse forcing and land ice) for more than 10,000 years until equilibration was achieved. From year 1765 to 1950, historical CO_2 forcing and geostrophically adjusted wind anomalies are applied. From 1950 to 2100, the model is forced with a combination of historical CO_2 forcing (to 2005) and a business-as-usual high atmospheric CO_2 concentration projection (Representative Concentration Projection 8.5 (refs. 30, 31), Extended Data Fig. 4). Global cumulative emissions have continued to track this scenario over recent years[32]. Atmospheric CO_2 concentrations are maintained at the year 2100 level for the duration of the simulations.

The large uncertainties still inherent in our understanding of global microplastic fate and transport necessitate the application of Latin Hypercube methodology[33] for its simulation. In ref. 4, 300 parameter combinations were used to force the model in 300 unique simulations between the years 1950 and 2100. Microplastic emissions start in year 1950 and follow a compound rate of increase of 8.4% per year[34], with the maximum potential pollution rate tuned to fall close to the 275 million metric tonnes of plastic waste generated by coastal countries at year 2010[35]. In ref. 4, a range of microplastic input fractions from 0% to 40% of maximum total plastic waste generated were applied (note that this is incorrectly stated in ref. 4 as a fraction of production, personal communication) after applying a mass conversion from tons to number of microplastic particles from ref. 36. Microplastic pollution rates exceeding 40% of coastal countries' total plastic waste generation are excluded on the basis of ref. 35 estimating about 4% of coastal countries' plastic waste generated is mismanaged but ref. 37 hypothesizing pollution rates are underestimated. Of the 300 Latin Hypercube simulations, only about half produced numerically stable simulations. The number of simulations were further reduced using the following criteria[4]:

- Microplastic pollution inventories exceeding 9×10^{14} particles at year 2010 are excluded on the basis of an independent estimate (3×10^{12} particles)[38] plus a 1–2 orders of magnitude assumed subsurface inventory, although noting upward revision of this upper limit to the assumed inventory may be considered in the future on the basis of new findings of high subsurface concentrations of small-size microplastics around gyres[39].
- Marine snow aggregation rates exceeding 10% are excluded based on the 3–5% estimate of ref. 40

These criteria reduced the sample size to 14 individuals from which three representatives were selected for detailed analysis. They were labelled as High Concentration, Medium Concentration and Low Concentration after their relative upper ocean microplastic inventories in our previous studies[4,5]. The biogeochemical consequences of zooplankton consuming microplastic in these three individual simulations were previously reported in ref. 5. The complete 14-member model ensemble demonstrated a robust additional loss of ocean oxygen due to zooplankton ingestion of microplastic pollution. This loss arises when zooplankton consume microplastic, even when microplastic is not a preferred food source, and for the whole range of values assigned to the other microplastic model parameters. A comparison model that does not include biological interaction with microplastic was also integrated (CNTL). In this manuscript, only the Medium Concentration and CNTL simulations are presented because committed biogeochemical model responses were very similar across model configurations. This is because microplastic pollution is applied only to the year 2022, after which the recovery depends entirely on model physics. The microplastic model presented here assumes that 27.6% of the fraction of annually

generated plastic waste by coastal countries ends up as microplastic in the ocean, that 1.1% of that microplastic will rise with positive buoyancy, that 52.8% of the microplastic ballasted by biological particles to the seafloor will return to the water column and that 9.2% of organic particles form marine snow aggregates. It furthermore assumes that zooplankton have a relative grazing selectivity of 0.193 for microplastic, that the food-to-microplastic conversion ratio is 0.993 and that the marine snow aggregation uptake constant for microplastic is 615.508. Please see ref. 4 for more details and a thorough exploration of the microplastic parameter space. Results of an alternative parameter configuration, using a much smaller microplastic pollution rate of 4% of the annually generated plastic waste by coastal countries[35], is presented as Extended Data Fig. 3.

Model configurations in the present study are summarized in Extended Data Table 1. In this study, microplastic pollution is ceased at year 2022 (Extended Data Fig. 4) while atmospheric CO_2 forcing continues. All microplastic concentrations in the ocean are also removed at year 2022. The models are integrated to year 3000 to investigate the long-timescale response of ocean biogeochemistry to microplastic pollution, as is committed to at year 2022. An ideal age tracer[41] is used to record the amount of time since water parcels last reach the ocean surface and is activated at year 1950 in the CNTL simulations. A set of comparison 'business-as-usual' simulations are also integrated, which maintain a 8.4% per year increase in microplastic pollution rate to year 2100, after which the pollution rate is held constant. Another set of comparison simulations that cease and remove microplastic pollution at year 2022, but for which sea ice does not inhibit air–sea O_2 exchange, are also provided to estimate the effect of sea ice on the trapping of the deoxygenation signal. We adopt the abbreviations MP_{BAU} ('business-as-usual' continued microplastics and climate forcing), MP_{STOP} (microplastics pollution ceased and all microplastics removed from the ocean at year 2022 but 'business-as-usual' climate forcing) and MP_{NOICE} (microplastics pollution ceased and all microplastics removed from the ocean at year 2022 and 'business-as-usual' climate forcing, but sea ice does not prevent air–sea oxygen exchange). These simulations are compared with CNTL and $CNTL_{NOICE}$, which account only for changes to the environment from 'business-as-usual' climate forcing.

Data availability

Model data are available at: https://zenodo.org/record/6640610#.YqgrE-xBw-Q

Code availability

Model code is available at: https://zenodo.org/record/6640610#.YqgrE-xBw-Q

References

18. Weaver, A. et al. The UVic Earth System Climate Model: model description, climatology, and applications to past, present and future climates. *Atmos. Ocean* **39**, 361–428 (2001).
19. Eby, M. et al. Lifetime of anthropogenic climate change: millennial time scales of potential CO_2 and surface temperature perturbations. *J. Clim.* **22**, 2501–2511 (2009).
20. Keller, D. P., Oschlies, A. & Eby, M. A new marine ecosystem model for the University of Victoria Earth System Climate Model. *Geosci. Model Dev.* **5**, 1195–1220 (2012).
21. Kvale, K., Meissner, K., Keller, D., Schmittner, A. & Eby, M. Explicit planktic calcifiers in the University of Victoria Earth System Climate Model, version 2.9. Atmos. Ocean https://doi.org/10.1080/07055900.2015.1049112 (2015).
22. Manno, C., Stowasser, G., Enderlein, P., Fielding, S. & Tarling, G. A. The contribution of zooplankton faecal pellets to deep-carbon transport in the Scotia Sea (Southern Ocean). *Biogeosciences* **12**, 1955–1965 (2015).
23. Min, K., Cuiffi, J. D. & Mathers, R. T. Ranking environmental degradation trends of plastic marine debris based on physical properties and molecular structure. *Nat. Commun.* **11**, 727 (2020).
24. Lebreton, L., Egger, M. & Slat, B. A global mass budget for positively buoyant macroplastic debris in the ocean. *Sci. Rep.* **9**, 12922 (2019).
25. Dey, S., Rout, A. K., Behera, B. K. & Ghosh, K. Plastisphere community assemblage of aquatic environment: plastic–microbe interaction, role in degradation and characterization technologies. *Environ. Microbiomes* **17**, 32 (2022).
26. Reisser, J. et al. Millimeter-sized marine plastics: a new pelagic habitat for microorganisms and invertebrates. *PLoS ONE* **9**, e100289 (2014).
27. Cole, M. et al. Microplastic ingestion by zooplankton. *Environ. Sci. Technol.* **47**, 6646–6655 (2013).
28. Cole, M., Lindeque, P., Fileman, E., Halsband, C. & Galloway, T. S. The impact of polystyrene microplastics on feeding, function and fecundity in the marine copepod *Calanus helgolandicus*. *Environ. Sci. Technol.* **49**, 1130–1137 (2015).
29. Courtene-Jones, W., Quinn, B., Ewins, C., Gary, S. F. & Narayanaswamy, B. E. Microplastic accumulation in deep-sea sediments from the rockall trough. *Mar. Pollut. Bull.* **154**, 111092 (2020).
30. Riahi, K., Gruebler, A. & Nakicenovic, N. Scenarios of long-term socio-economic and environmental development under climate stabilization. *Technol. Forecasting Social Change* **74**, 887–935 (2007).
31. Meinshausen, M. et al. The RCP greenhouse gas concentrations and their extensions from 1765 to 2300. *Climatic Change* **109**, 213–241 (2011).
32. Schwalm, C. R., Glendon, S. & Duffy, P. B. RCP8.5 tracks cumulative CO_2 emissions. *Proc. Natl Acad. Sci. USA* **117**, 19656–19657 (2020).
33. McKay, M. D., Beckman, R. J. & Conover, W. J. A comparison of three methods for selecting values of input variables in the analysis of output from a computer code. *Technometrics* **21**, 239–245 (1979).
34. Geyer, R., Jambeck, J.R. & Law, K.L. Production, use, and fate of all plastics ever made. Sci. Adv. https://doi.org/10.1126/sciadv.1700782 (2017).
35. Jambeck, J. R. et al. Plastic waste inputs from land into the ocean. *Science* **347**, 768–771 (2015).
36. van Sebille, E. et al. A global inventory of small floating plastic debris. *Environ. Res. Lett.* **10**, 124006 (2015).
37. Kvale, K., Friederike Prowe, A. E. & Oschlies, A. A critical examination of the role of marine snow and zooplankton fecal pellets in removing ocean surface microplastic. *Front. Mar. Sci.* **6**, 808 (2020).
38. Eriksen, M. et al. Plastic pollution in the world's oceans: more than 5 trillion plastic pieces weighing over 250,000 tons afloat at sea. *PLoS ONE* **9**, e111913 (2014).
39. Zhao, S. et al. Large quantities of small microplastics permeate the surface ocean to abyssal depths in the South Atlantic gyre. *Glob. Change Biol.* **28**, 2991–3006 (2022).
40. Shanks, A. & Trent, J. Marine snow: sinking rates and potential role in vertical flux. *Deep Sea Res. Part A* **27**, 137–143 (1980).
41. Koeve, W., Wagner, H., Kähler, P. & Oschlies, A. ^{14}C-age tracers in global ocean circulation models. *Geosci. Model Dev.* **8**, 2079–2094 (2015).

Acknowledgements

We would like to acknowledge computer resources made available by Kiel University. K.K. acknowledges support from the New Zealand Ministry of Business, Innovation and Employment within the Antarctic Science Platform, grant ANTA1801. K.K. also acknowledges support from the New Zealand Ministry of Business, Innovation and Employment (MBIE) through the Global Change through Time programme (Strategic Science Investment Fund, contract C05X1702).

Figure plotting used the Ferret plotting programme. Ferret is a product of the US National Oceanic and Atmospheric Administration's Pacific Marine Environmental Laboratory.

Author contributions

A.O. proposed the study. K.K. ran the simulations and wrote the paper. Both authors edited the manuscript.

Competing interests

The authors declare no competing interests.

Additional information

Extended data is available for this paper at https://doi.org/10.1038/s41561-022-01096-w.

Supplementary information The online version contains supplementary material available at https://doi.org/10.1038/s41561-022-01096-w.

Correspondence and requests for materials should be addressed to Karin Kvale or Andreas Oschlies.

Peer review information *Nature Geoscience* thanks Atsuhiko Isobe and Anthony Richardson for their contribution to the peer review of this work. Primary Handling editor: Rebecca Neely, in collaboration with the Nature Geoscience team.

 https://doi.org/10.1038/s41561-022-01096-w

Extended Data Table 1 | Simulation configurations

Configuration	Climate forcing	Microplastic forcing	Air-sea gas exchange through sea ice
CNTL	yes	no	no
$CNTL_{NOICE}$	yes	no	yes
MP_{STOP}	yes	not after 2022	no
MP_{BAU}	yes	yes	no
MP_{NOICE}	yes	not after 2022	yes
$CNTL_{LOSS}$	yes	no	ocean degassing only
$CNTL_{GAIN}$	yes	no	ocean uptake only

https://doi.org/10.1038/s41561-022-01096-w

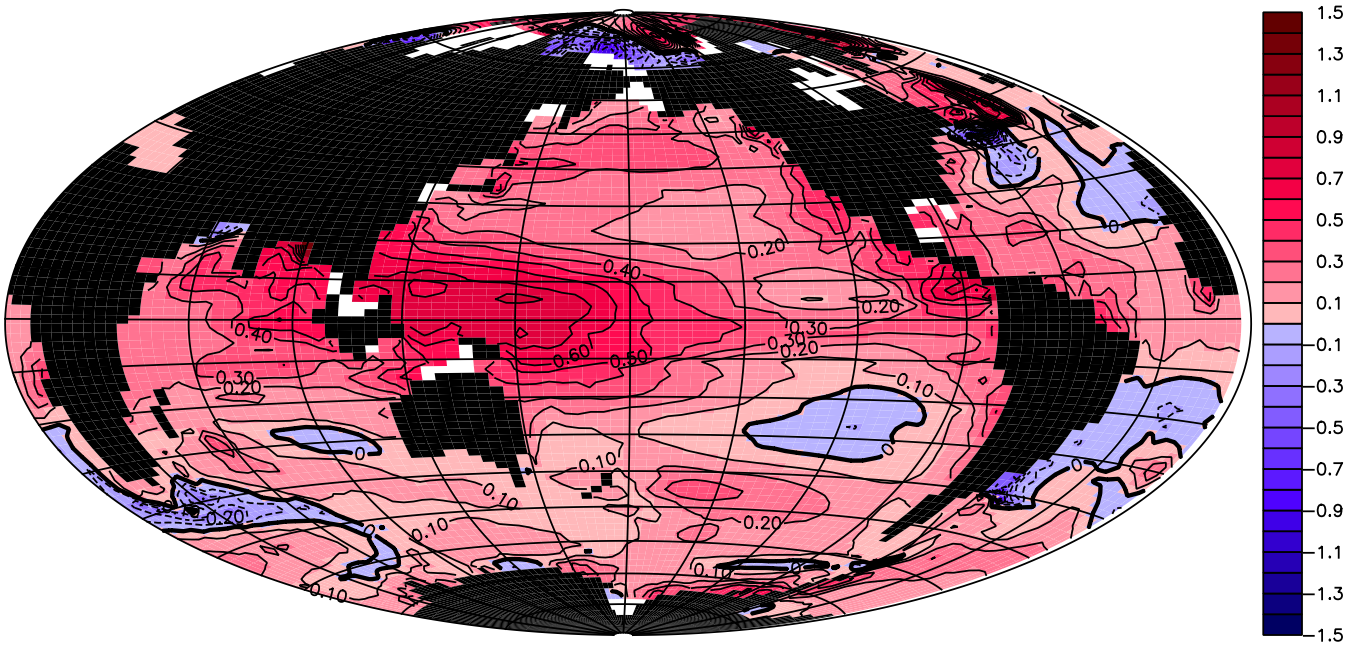

Extended Data Fig. 1 | Ocean surface stratification trends between years 2022 and 2200. Stratification is approximated as the change in density from the surface to 300 m depth. Units are kg m^{-3}.

https://doi.org/10.1038/s41561-022-01096-w

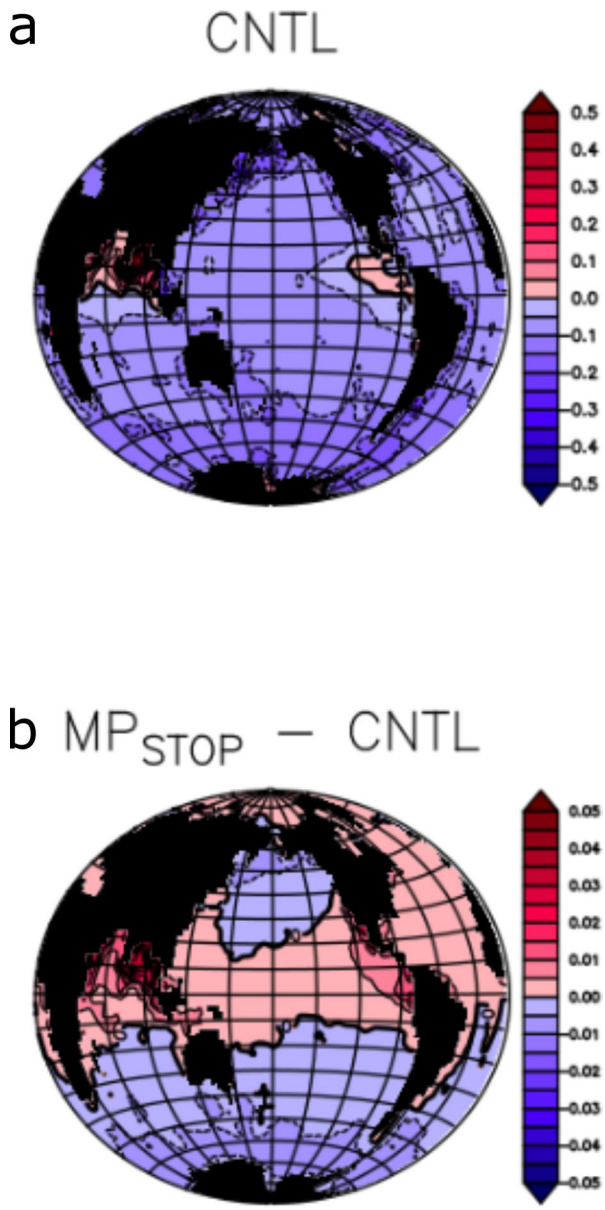

Extended Data Fig. 2 | Changes in the average water column metabolic index[9]. A metabolic index is defined as the ratio of oxygen supply to the temperature-dependent resting oxygen demand of an organism. Here it is applied generically as an indicator of the change in metabolic viability of an environment using average parameters from[9]. Panel a, Change in the metabolic index due to climate warming at year 2200, relative to year 2022. Panel b, change in the metabolic index due to historic microplastic pollution at year 2200, relative to year 2022.

https://doi.org/10.1038/s41561-022-01096-w

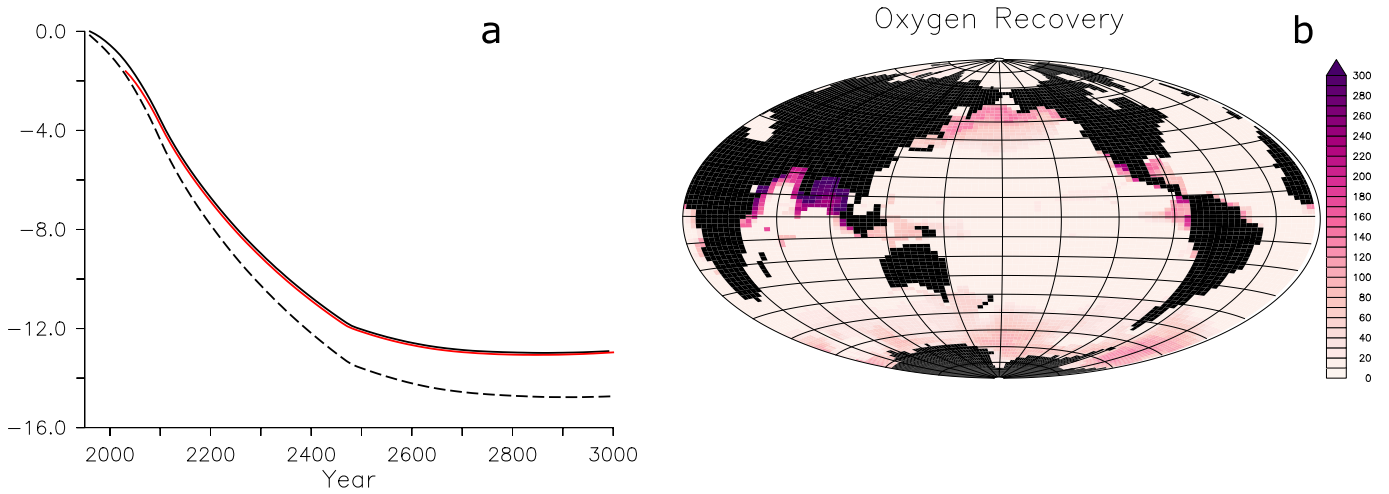

Extended Data Fig. 3 | Oxygen recovery using a lower pollution rate. Panel a, Timeseries of global oxygen loss as a percentage relative to value at year 1950 due to climate change (solid black line), ongoing microplastic pollution (dashed black line), and microplastic removal (red line) using a low rate of plastic pollution. Panel b, Timescale in years of average water column oxygen recovery to within 1% of the climate change-only value using a low rate of plastic pollution.

https://doi.org/10.1038/s41561-022-01096-w

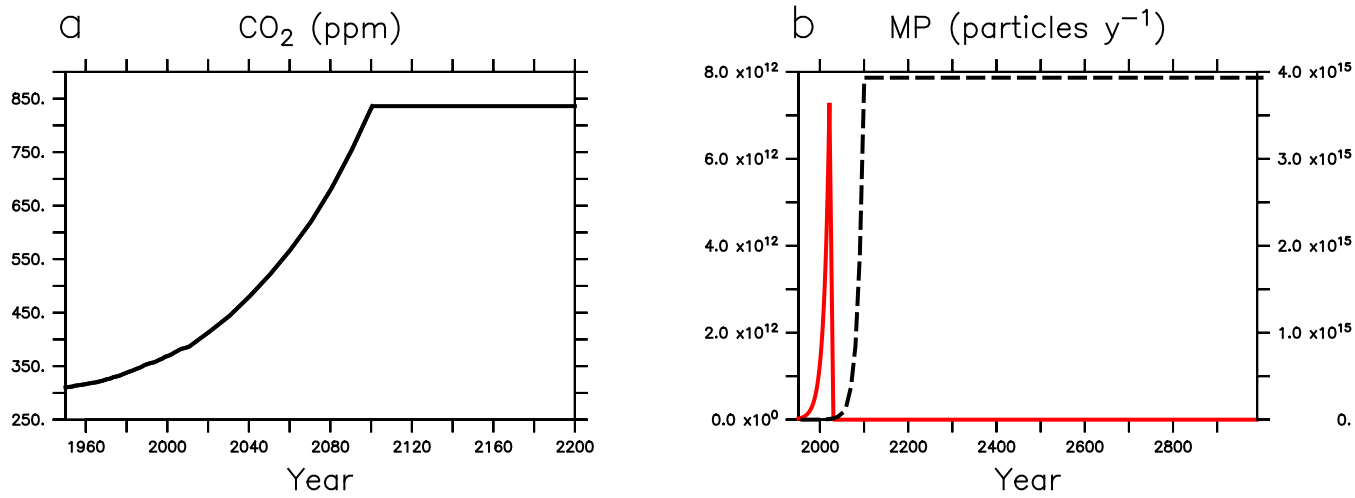

Extended Data Fig. 4 | Model forcing. Panel a, RCP8.5 atmospheric CO_2 concentration forcing. Panel b, All ocean microplastic is removed at year 2022, and pollution stopped, in MP_{STOP} (red line, left axis). Microplastic pollution continues to rapidly increase to year 2100 in MP_{BAU} (black dashed line, right axis).